
Article:
Pittiglio, G, Barducci, L, Martin, JW et al. (2019) Magnetic Levitation for Soft-Tethered Capsule Colonoscopy Actuated With a Single Permanent Magnet: A Dynamic Control Approach. IEEE Robotics and Automation Letters, 4 (2). pp. 1224-1231. ISSN: 2377-3766

https://doi.org/10.1109/LRA.2019.2894907

Magnetic Levitation for Soft-Tethered Capsule Colonoscopy Actuated with a Single Permanent Magnet: a Dynamic Control Approach

Giovanni Pittiglio[1], Lavinia Barducci[1], James W. Martin[1], Joseph C. Norton[1], Carlo A. Avizzano[2], Keith L. Obstein[3], and Pietro Valdastri[1]

***Abstract*—The present paper investigates a novel control approach for magnetically driven soft-tethered capsules for colonoscopy - a potentially painless approach for colon inspection. The focus of this work is on a class of devices composed of a magnetic capsule endoscope actuated by a single external permanent magnet. Actuation is achieved by manipulating the external magnet with a serial manipulator, which in turn produces forces and torques on the internal magnetic capsule. We propose a control strategy which, counteracting gravity, achieves levitation of the capsule. This technique, based on a nonlinear backstepping approach, is able to limit contact with the colon walls, reducing friction, avoiding contact with internal folds and facilitating the inspection of non-planar cavities. The approach is validated on an experimental setup which embodies a general scenario faced in colonoscopy. The experiments show that we can attain 19.5 % of contact with the colon wall, compared to the almost 100 % of previously proposed approaches. Moreover, we show that the control can be used to navigate the capsule through a more realistic environment - a colon phantom - with reasonable completion time.**

***Index Terms*—Medical Robots and Systems, Force Control, Motion Control.**

I. Introduction

OVER the last decade, magnetically actuated robotic platforms have had a significant impact in the field of medical robotics, providing new tools to facilitate minimally invasive diagnosis and therapy in different regions of the human body. The main advantage of magnetically actuated robots is the application of functional forces and torques without the need for the alternative, often complex and bulky on-board locomotion mechanisms. Due to this advantage, these devices have been investigated for several endoscopic procedures such as *colonoscopy* [1], [2], [3], *gastroscopy* [4], *cardiac applications* [5], [6], [7], [8], [9], *surgery* [10] and *bronchoscopy* [11].

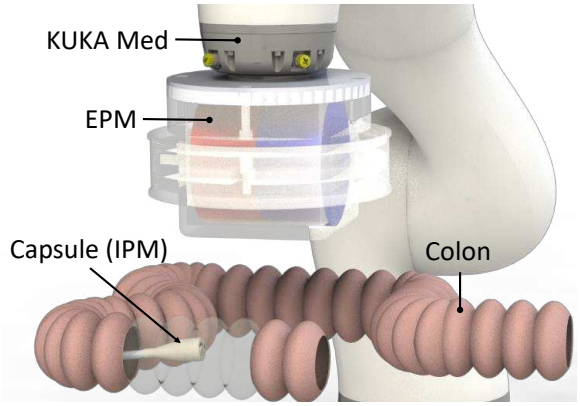

Figure 1. Schematic representation of the platform.

In general, magnetically actuated endoscopic robots can be subdivided in terms of external actuation, between *coil-based* [12], [13], [5], [14], [15], [16], [17], *rotating permanent magnets-based* [18], [19] and *permanent magnet-based* [1], [2], [3], [4], [20] devices. The first ones generate a magnetic field, generally, based on the usage of multiple coils within a predefined workspace. The second ones make use of rotating magnets instead of coils. Permanent magnet-based devices are actuated by a single permanent magnet, manipulated by a serial robot.

Systems that use multiple coils generally have higher controllability owing to the fine control over the magnetic field within the workspace. However, these systems are often more bulky, have a confined workspace, are expensive and have a high energy consumption that may hinder their practical use.

Rotating permanent magnets-based devices, permit 6 Degrees of Freedom (DOFs) steering, when employing multiple magnets [19]. This approach avoids heating normally associ-

Manuscript received: September, 10, 2018; Revised December, 12, 2018; Accepted January, 12, 2019.

This paper was recommended for publication by Editor P. Rocco upon evaluation of the Associate Editor and Reviewers' comments.

This research was supported by the Royal Society, UK under grant number CH160052, by the Engineering and Physical Sciences Research Council, UK under grant number EP/P027938/1 and EP/K034537/1, by the National Institute of Biomedical Imaging and Bioengineering, USA of the National Institutes of Health under award no. R01EB018992 and by the Italian Ministry of Health funding programme "Ricerca Sanitaria Finalizzata 2013 - Giovani Ricercatori" project n. PE-2013-02359172. Any opinions, findings, conclusions, or recommendations expressed in this material are those of the authors and do not necessarily reflect the views of the Royal Society, the Engineering and Physical Sciences Research Council, the National Institutes of Health or the Italian Ministry of Health.

G. Pittiglio and L. Barducci contributed equally to this work.

[1]G. Pittiglio, L. Barducci, J. W. Martin, J. C. Norton and P. Valdastri are with the STORM Lab UK, School of Electronic and Electrical Engineering, University of Leeds, Leeds, UK. {g.pittiglio, ellb, eljm, j.c.norton, p.valdastri}@leeds.ac.uk.

[2]C. A. Avizzano is with PERCeptual RObotics Laboratory, Scuola Superiore SantAnna, Pisa, Italy. c.avizzano@sssup.it

[3]K. L. Obstein is with the Division of Gastroenterology, Hepatology, and Nutrition, Vanderbilt University Medical Center, Nashville, TN, USA, and with the STORM Lab, Department of Mechanical Engineering, Vanderbilt University, Nashville, TN, USA keith.obstein@vanderbilt.edu

Digital Object Identifier (DOI): see top of this page.

ated with using coils, but shares the same limitations in terms of workspace.

The focus of the present work is Magnetic Flexible Endoscope (MFE) actuated with single External Permanent Magnet (EPM) [1], [3], shown in Fig. 1. This has been investigated as an alternative to standard colonoscopy, with the main advantages of being ease-of-use and reduced patient discomfort - two significant drawbacks with the current procedure. Standard colonoscopes, pushed from outside the body, advance through the colon by exerting pressure on the bowel wall. This environmental interaction is needed to steer the device and conform its shape to the tortuous lumen. On-the-other-hand, soft-tethered magnetic capsules are controlled by an externally applied force focused at the tip of the device. Therefore, in order to advance the capsule, there is no need to exert stress on the lumen; the forces are applied in the required direction only and the soft tether follows passively.

However, a potential limitation of this platform is the continuous attraction of the capsule to the EPM and lack of gravity compensation [21]. This may cause the capsule to become trapped in the anatomically complex and unstructured environment of the colon and may hinder locomotion through a steeply sloping lumen. The method in [21] is able only to control 4 DOFs: 2 DOFs on the plane, pitch and yaw. However, magnetic coupling between 2 single-dipole permanent magnets inherently permits the actuation of 5 DOFs; due to the cylindrical symmetry of the magnetic field, capsule roll is not possible. Therefore, the goal of our contribution is to enhance current practice by adding the actuation of the 5th DOF: the one along the gravity direction. This aims to reduce contact with the environment and facilitate locomotion. However, the fundamental challenge of the proposed approach is that the equilibrium between magnetic force and gravity is highly unstable and, therefore, the control design is nontrivial.

While levitation is technically easier to implement in coil-based systems [22], in this paper we aim to show that accurate control can be used to counter the limited controllability of systems with a single EPM. We show that levitation (controlling the capsule in the gravity direction) is feasible and can be done in free-space, i.e. without the need for a fluid medium [4]. This is relevant in the context of colonoscopy because the lumen is routinely distended with a gas medium. This control strategy can bring significant benefit as it facilitates the avoidance of obstacles (eg. tissue folds), a reduction in contact force and therefore, a reduction in both friction and risk of trauma or discomfort. It may also assist with navigating sloped regions of the colon.

This paper is organized as follows: in Section II we provide a general overview of the method, which is explored further in Section III. Sections IV and V present the experimental data, which aims to prove the strength of the proposed approach; the former discusses free space levitation in a L-shaped acrylic tube, the latter reports the results obtained in a more realistic colon phantom. Section VI draws our main conclusions and discusses future work. In Appendix A we give detail on the basics of magnetic manipulation and Appendix B reports proofs of lemmas and theorems employed in the paper.

II. Method

In the following we aim to describe a general approach for magnetic capsule levitation using a single EPM. The EPM is controlled by a serial manipulator and the capsule contains a magnet, referred to as Internal Permanent Magnet (IPM)[1]. This is shown in Fig. 1. Achieving accurate control with robotically actuated permanent magnets [4] is challenging, due largely to the high inertia related to the movements of the large EPM and serial manipulator, compared to current flow. Moreover, when considering only a single magnetic source, point-wise control of the magnetic field and its gradient is not as straightforward as in using multiple coils.

In order to achieve levitation we need to guarantee that the force on the IPM counteracts gravity, in an equilibrium state that is highly unstable. The approach taken can either be to design a controller aware of the dynamics of the IPM or to design a suitable trajectory planner that does not require the dynamic equilibrium to be considered. Our initial approach was to purse the latter and avoid the use of the system dynamics. As is shown in subsequent sections, this is a feasible approach that achieves asymptotic stability.

The overall control strategy is based on the *backstepping technique* and the global stability is formally proved by means of a Lyapunov-based approach [23]. This is guaranteed under the assumption that the desired trajectory of the IPM is a *piecewise-constant* function of the time. This means that desired velocity and acceleration of the IPM can be neglected. In this condition, a PD controller can be designed to steer the IPM and achieve asymptotic convergence. The assumption made does not interfere with the design of the controller, nor is limiting in any case when a smooth planning can be achieved.

This control technique uses capsule localization (100 Hz, 4 mm accuracy) [24], where the pose and inferred force and torque are known.

III. Dynamic Control

We take into account a *back-stepping* approach [23] on two levels (or loops): pose loop (Section III-A) and force loop (Section III-B). The latter, considered as an internal loop, is designed to guarantee the convergence of the actual force on the IPM to the desired one, while the former aims to steer the IPM. The presence of the internal force loop improves the control properties, compared to previous approaches [21], [4], and it is fundamental for levitation. Given the unstable force equilibrium, it is essential to guarantee the stability of this internal loop before attempting to steer the IPM. This control strategy is summarized in Fig. 2.

In this work, we only consider the dynamics of the capsule subject to forces and torques exerted by the EPM. These forces and torques, embedded in the vector $\tau_m \in \mathbb{R}^n$, depend on the relative position between the IPM and EPM, as described in the Appendix A. In general, $n = 5$ for single external magnetic source and $n = 6$ for multiple magnetic sources [14]. We consider that the two permanent magnets can be approximated with the *dipole model*, which is enough accurate

[1]In the following we use the name Internal Permanent Magnet also in reference to the magnetic capsule.

given their geometry and relative distance. Possible errors related to dipole modelling are discussed along with the experimental data provided in Sections IV. For the sake of clarity, we discuss any implication, mathematical operator and variable in Appendix A.

In the present work, the presence of a tether is considered an unmodelled disturbance. In the specific case under analysis, the tether is beneficial as it acts as a stabilizing damper on the dynamics along the gravity direction, improving stability in the system. There is no limitation in applying the proposed method to untethered capsules, but we expect the need for a faster control loop to handle the less damped dynamics.

Consider the nominal dynamics of the capsule

$$B(x)\ddot{x} + C(x,\dot{x})\dot{x} + G(x) = \tau_m(x,q), \tag{1}$$

where $x \in \mathbb{R}^n$ is the capsule pose (position and orientation) and $q \in \mathbb{R}^m$ embeds the robot joint variables; matrices $B(x)$, $C(x,\dot{x})$, $G(x)$ are the respective *inertia*, *Coriolis matrix* and *gravity* [25]. Our aim is to find q such that x approaches a desired value x_d.

The relationship $\tau_m(x,q)$ is the magnetic dipole force and torque exerted by the EPM on the IPM. This relationship is highly nonlinear, confounding computation of q given the desired force and torque on the IPM. Appendix A describes this in more detail. Therefore, we consider a time derivation of this function [21], which reads as

$$\dot{\tau}_m = \frac{\partial \tau(x,q)}{\partial x}\dot{x} + \frac{\partial \tau(x,q)}{\partial q}\dot{q} = J_x\dot{x} + J_q\dot{q}, \tag{2}$$

and turns τ_m into a state variable for the system we aim to control and $\dot{q}$ into the control input; matrices J_x and J_q are derived in the Appendix A. The variables $\dot{q}$ can be integrated to control the robot through its Direct Kinematics (DK) [25]. The novelty of our control system, compared to [21], is that we apply a closed-loop control on τ_m.

The overall dynamics we aim to control reads as

$$\begin{cases} B(x)\ddot{x} + C(x,\dot{x})\dot{x} + G(x) &= \tau \\ \dot{\tau} &= J_x\dot{x} + J_q\dot{q} + \dot{\nu} \end{cases}, \tag{3}$$

where ν models the tether interaction with the environment, for example: drag, elastic behaviour and friction; τ is the actual force and torque on the capsule. The localization method [24] ensures that x and $\dot{x}$ can be measured. The robot joints are measured by the embedded encoders.

In the following sections we describe the main steps in the derivation of the controller and conclude by proving the stability of the controlled system, using Lemma 1 and Theorem 1 (described in detail in Appendix B).

A. Pose Control

Defining a pose controller that attempts to steer the IPM to a desired trajectory (x_d) is the first step and is achieved by first considering that τ can be deliberately set as a control input for the upper dynamics in (3). Because of the nonlinearities described in Appendix A, we attempt to find a set of desired forces and torques (referred to as τ_d). Afterwards, as described in the next section, we aim to control the actual torque (τ) to

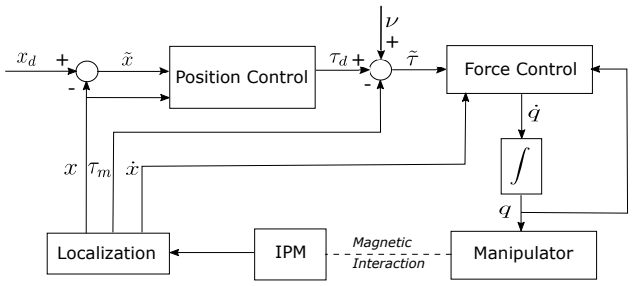

Figure 2. Control scheme.

τ_d. The stability of this backstepping approach, as shown in Section III-C, guarantees the overall convergence.

We want to prove that the *PD with gravity compensation*

$$\tau_d = G(x) + K_p\tilde{x} + K_d\dot{\tilde{x}}, \tag{4}$$

with $\tilde{x} = x_d - x$, guarantees $x \to x_d$ as $\tau \to \tau_d$. This is achieved under the following assumption.

Assumption 1: The steering of the IPM is achieved by considering that:

- the force control, described in Section III-B, is faster than the system dynamics in (1);
- the desired trajectory is a *piece-wise constant function of the time*.

The former leads to assume that there exists an instant T, $0 < T \ll 1$, such that $\tau(t) = \tau_d(t)$, $t \geq T$. In other words, we consider almost instantaneous convergence of force and torque. This simplification is used to prove the first step of the backstepping; Section III-C discusses the case of a weaker assumption. The need for this assumption is justified by the following lemma, on which the final proof of this work (Theorem 1) is based.

Lemma 1: Under Assumption 1, the pose controller in (4) achieves asymptotic stability of the error $\tilde{x}$, for any positive definite design gains K_p and K_d.
Appendix II includes further details on this.

B. Force Control

The second step in the design of the controller is to ensure that τ converges to τ_d and do so almost instantaneously (according to Assumption 1). The magnetic force and torque are computed from x and q by employing the localization data and dipole model.

In order to design an asymptotically stable controller for force and torque, we take into account (2) and search for $\dot{q}$ such that the dynamics for $\tilde{\tau} = \tau_d - \tau_m$ evolves as

$$\dot{\tilde{\tau}} = -K\tilde{\tau}, \tag{5}$$

with K positive definite design gain. This leads to asymptotic stability of the force and torque error dynamics.

By substituting (2) into (5) we obtain

$$\dot{\tau}_d - \dot{\tau}_m = -K\tilde{\tau}$$
$$\dot{\tau}_d - J_x\dot{x} - J_q\dot{q} = -K\tilde{\tau}$$

whose solution, with respect to $\dot{q}$, is

$$\dot{q} = J_q^{\dagger}(\dot{\tau}_d + K\tilde{\tau} - J_x\dot{x}). \tag{6}$$

Here $(\cdot)^\dagger$ stands for the *Moore-Penrose pseudoinverse* [25]. Note that the derivative of the desired torque τ_d can be analytically computed from the localization data, by following the steps in Appendix A.

Lemma 2: Under the assumption that the disturbance $\nu \simeq 0$, any positive definite gain K achieves stability of the torque dynamics.

Proof: Under the drawn assumption, $\tau \simeq \tau_m \to \tau_d$. ■

Assuming the tether interactions to be negligible is justified by the fact that the tether used in our platform interacts with the environment with a very low friction coefficient - the tether and colon are both smooth and lubricated. Furthermore, considering that the tether is significantly stiffer than the colon, the elastic restoring forces would have minimal impact on capsule dynamics and any deformation would be seen primarily in the wall of the colon.

C. Overall Control

In the following, we describe the overall control strategy by considering the above results. In particular, we show that with the choice of $\dot{q}$

$$\begin{cases} \tau_d &= G(x) + K_p\tilde{x} + K_d\dot{\tilde{x}} \\ \dot{q} &= J_q^\dagger(\dot{\tau}_d + K\tilde{\tau} - J_x\dot{x} - \dot{x}) \end{cases}, \tag{7}$$

we can weaken Assumption 1. The new choice of $\dot{q}$ leads to

$$\dot{\tilde{\tau}} = -K\tilde{\tau} + \dot{x},$$

which achieves overall convergence, as discussed in Theorem 1. Therefore, the assumption under which we guarantee the overall convergence of the controlled system is the following.

Assumption 2: The desired trajectory x_d is *piece-wise constant function* of the time and $\nu \simeq 0$.

We can prove the convergence of the controlled dynamics, as in the following theorem.

Theorem 1: Under Assumption 2, the controller defined in (7) achieves asymptotic stability of the dynamics (3), for any positive definite design gains K_p, K_d and K.
This is elaborated in Appendix B.

IV. Experimental Analysis: Free Space Levitation

The aim of the experimental work was to show that we can achieve levitation, including steering the capsule through inclined trajectories. This could be an essential tool for facilitating effective locomotion in the presence of obstacles and complex colon geometries. A video of the experiments is reported in the attached media of the paper.

The IPM was first placed into an acrylic tube with a realistic inner diameter of 60 mm [26], bent at an angle of 90 degrees in the center. Each half of the tube was 250 mm long. The tube was inclined by approximately 20 mm over its length. This was chosen to show our controller performance when moving the capsule along the gravity direction (x_3).

The IPM (axially magnetized, 21 mm diameter, 19 mm length, 15 g mass) is actuated using an EPM (axially magnetized, 101.6 mm diameter and length, 1.48T, N52) at the End Effector (EE) of a serial manipulator (KUKA LBR Med R820[2]). Localization [24] and control loop both run at approximately 100 Hz. The error in the dipole models were computed by considering [27] and the conditions during experiments. For the EPM, the maximum and mean error were 13 % and 3 % respectively. Whereas the corresponding errors for the IPM were 0.2 % and 0.06 % respectively. Magnetic interference was minimized by keeping the workspace free from ferromagnetic materials.

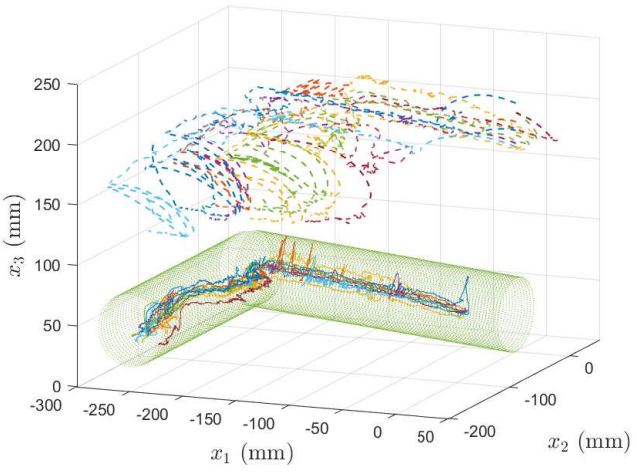

Figure 3. 3D tracking. The IPM (solid line) and EPM (dashed line) trajectories for all trials performed.

To show the efficacy of the control strategy, we commanded the capsule to traverse the acrylic tube in 10 trials. We report the 3D trajectories of the IPM and EPM in Fig. 3. The mean force along the gravity direction (τ_3), measured throughout the trajectories, is shown in Fig. 4(a). The mean distance between the capsule and the center of the tube (D), is shown in Fig. 4(b). These both give an indication of the levitation performance; in-other-words, how effectively the system prevents the capsule from touching the surrounding walls.

We controlled the capsule to be in the center of the lumen on the x_1-x_2 plane while maintaining the minimum height on the axis x_3 which achieves levitation - i.e. where τ_3 counteracts gravity. In the first part of the tube, this objective translates directly into levitating the capsule, as shown in Fig. 3. On-the-other-hand, in the second half of the path, the stiffness of the tether and acrylic tube leads to capsule-tube contact because of their large resistance to deformation. In this case the EPM is not able to exert enough force to counteract this resistance. Although the tether properties negatively impact simultaneous steering and levitation, the experiments show that the control strategy can resume capsule levitation after moving past the corner.

Fig. 4(b) quantifies the amount of contact with the internal wall. The event of the capsule touching the wall is quantified by geometric constraints and real-time localization. The latter provides information about the position of the capsule inside the acrylic tube (upon an initial registration). The result is that,

[2]https://www.kuka.com/en-gb/industries/health-care/kuka-medical-robotics

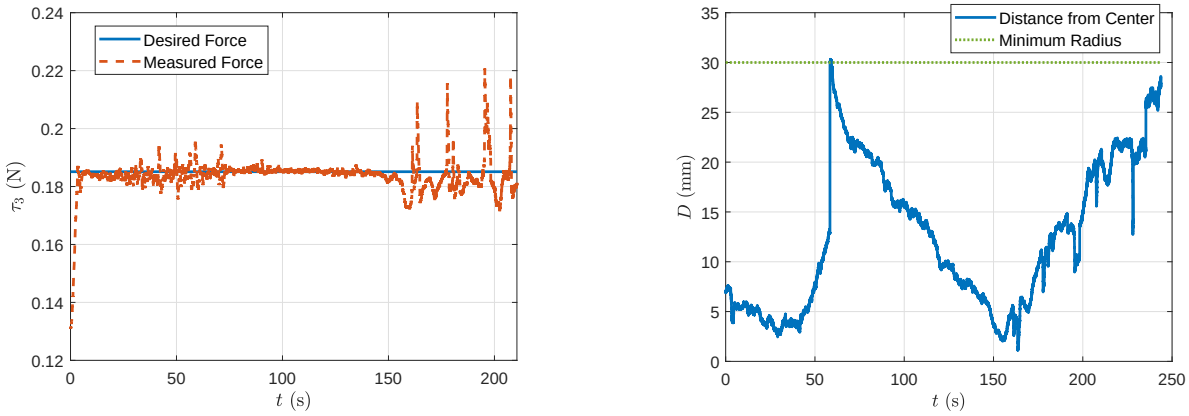

(a) Mean levitating force.

(b) Mean distance from wall.

Figure 4. Evaluation of levitating performance.

on average, the capsule is in contact with the tube 19.5 % of the time, compared to almost 100 % for previous methods [21]. Less contact with the environment can be equated to smoother locomotion.

V. Experimental Analysis: Colon Phantom

In the following we describe an experiment performed on the M40 Colonoscope Training Simulator[3] in *standard configuration*. The aim was to show that the proposed method is able to control the IPM in a more realistic environment that is deformable, unstructured and contains obstacles. While quantitative feedback on capsule-environment contact could not be measured in this setup, the results show the feasibility of pursuing this control strategy.

These tests also validate our assumption of considering the tether dynamics as a disturbance, as the capsule is able to successfully traverse the complex environment despite tether-environment interaction. The colon has a low stiffness and provides little resistance to deformation from the comparatively stiffer tether.

We performed 5 trials in which the user (an individual with no prior endoscopic experience, but knowledge of the system) was tasked with traversing the colon phantom from sigmoid to ceacum. The user was provided with visual feedback from the capsule's on-board camera and could manipulate the capsule pose using a 3D mouse. This setup is shown in Fig. 5.

In Fig. 6 we show the colon phantom with all 5 trajectories overlaid. An example of one of these trials can be seen in the supplementary media attachment.

The overall task had a mean completion time of 346.78 s with standard deviation of 119.37 s, for a path of approximately 0.85 m. This would equate to exploring a typical human colon in approximately 13 min, assuming an average colon length of 1.85m [26] and a mean capsule velocity of 2 mm/s seen in these experiments. In order to investigate the real performance of the proposed approach, a deeper analysis will be performed with expert users, as in [1].

[3]https://www.kyotokagaku.com/products/detail01/m40.html

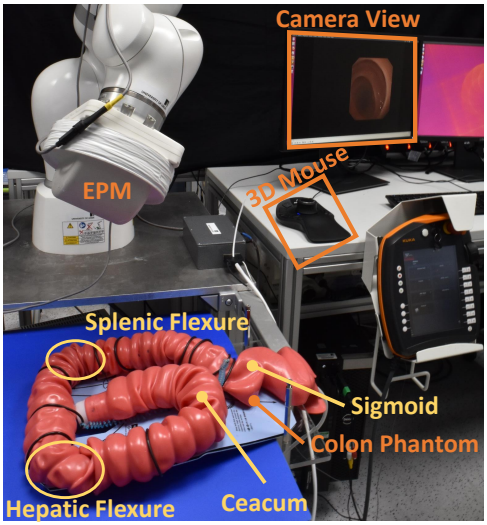

Figure 5. Experimental setup: colon simulator.

Increasing the velocity is related to two factors: the frequency of the control loop and the need for Assumption 2. The current localization frequency (100 Hz) is not fast enough to guarantee the capsule dynamics are handled completely and so increasing this would have a direct impact on system performance. Assumption 2 can be overcome by performing techniques which consider the system dynamics. These will be explored in future work.

VI. Conclusions

The present paper discussed a novel control technique for capsule levitation in magnetically driven capsule colonoscopy. This was motivated by the potential benefits of reduced friction, and obstacle avoidance, for improved locomotion in complex environments such as the colon. This is important as locomotion in this context is extremely challenging; devices are prone to becoming trapped in the soft folds of tissue and friction/drag can hinder progress. Although the magnetic system is inherently gentle, deforming the environment very

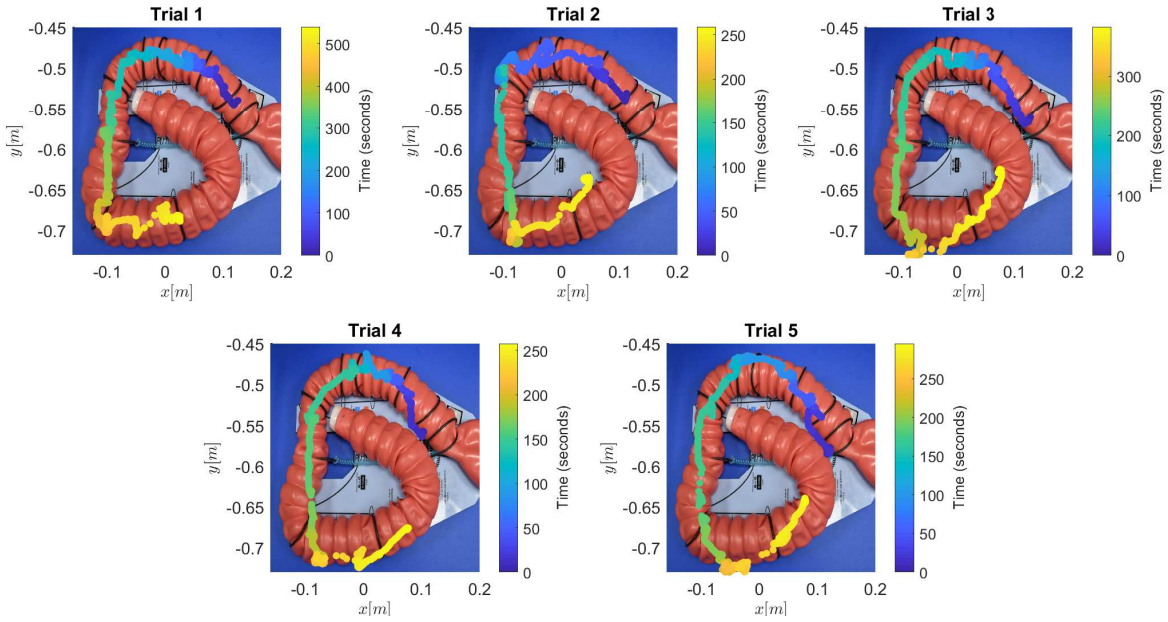

Figure 6. Trials on the colon simulator.

little, the proposed control strategy improves this further and so may reduce clinical risks and patient discomfort. The control strategy is based on a gravity compensation approach which attains capsule levitation and fine control along the gravity direction, while also permitting capsule steering.

The asymptotic stability of the proposed technique was proved by employing the Lyapunov approach and supported in the experimental results from tests in an acrylic tube. These results show that, while levitating, we are able to handle slopes and, compared to previous solutions, reduce contact with the cavity from approximately 100 % to 19.5 %. On the base of these results, we can conclude that the control approach is a promising technique for general application in magnetically driven capsule colonoscopy.

In order to strengthen this inference, we also performed colonoscopy on a phantom simulator for colonoscopy training. These results show that we can perform colonoscopy by employing the levitation technique. Due to the encouraging results obtained in the colon phantom, we aim to confirm our findings in more realistic experimental settings (i.e. animal and cadaver models) in the near future. Moreover, we will investigate the possibility of using the solely levitation or any combination of it with other control techniques.

One of the current limitations of the present work is assuming that tether-environment interactions are negligible disturbances. In our future works, we will also investigate how to integrate these interactions in out control scheme, possibly by embedding real-time shape sensors inside the tether.

APPENDIX A
MAGNETIC ACTUATION

In this appendix, we aim to discuss some basic concepts about magnetic actuation and define some of the variables used in the paper. We consider that both IPM and EPM can be modelled as dipoles and recall some of the implications already discussed in [21]. We show how to compute the magnetic force $\tau_m(x,q)$ and how magnetism relates to the dynamics in (1).

Consider the pose of the EE of the robot being referred to as $\chi \in \mathbb{R}^n$ and introduce the vector between EE position p_E (or, equivalently, EPM) and IPM position p_I as $p = p_E - p_I$. We consider the robot EE being the EPM. The force and torque between the two magnets can be expressed as

$$\tau_m = \begin{pmatrix} \frac{3\lambda}{||p||}(\hat{m}_E\hat{m}_I^T + \hat{m}_I\hat{m}_E^T + (\hat{m}_I^T Z \hat{m}_I)I)\hat{p} \\ \lambda \hat{m}_I \times D\hat{m}_E \end{pmatrix}$$

where

$$\lambda = \frac{\mu_0 ||m_I||\ ||m_E||}{4\pi ||p||^3},$$

$m_I = ||m_I||\hat{m}_I$ and $m_E = ||m_E||\hat{m}_E$ are the respective *magnetic moments* of IPM and EPM, $\hat{p} = \frac{p}{||p||}$, $Z = I - 5\hat{p}\hat{p}^T$ and $D = 3\hat{p}\hat{p}^T - I$; here $I \in \mathbb{R}^{3\times 3}$ is referred to as the *identity matrix* and $||\cdot||$ is the *Euclidean norm*.

As in [21], we consider the time derivative of τ_m

$$\begin{aligned}\dot{\tau}_m &= \begin{pmatrix} \frac{\partial \tau}{\partial p} & \frac{\partial \tau}{\partial \hat{m}_E} & \frac{\partial \tau}{\partial \hat{m}_I} \end{pmatrix} \begin{pmatrix} \dot{p} \\ \dot{\hat{m}}_E \\ \dot{\hat{m}}_I \end{pmatrix} \\ &= \begin{pmatrix} \frac{\partial \tau}{\partial p} & \frac{\partial \tau}{\partial \hat{m}_E} & \frac{\partial \tau}{\partial \hat{m}_I} \end{pmatrix} \left[\begin{pmatrix} \dot{p}_E \\ \dot{\hat{m}}_E \\ 0 \end{pmatrix} - \begin{pmatrix} \dot{p}_I \\ 0 \\ \dot{\hat{m}}_I \end{pmatrix} \right] \\ &= \begin{pmatrix} \frac{\partial \tau}{\partial p} & \frac{\partial \tau}{\partial \hat{m}_E} \end{pmatrix} \begin{pmatrix} \dot{p}_E \\ \dot{\hat{m}}_E \end{pmatrix} - \begin{pmatrix} \frac{\partial \tau}{\partial p} & \frac{\partial \tau}{\partial \hat{m}_I} \end{pmatrix} \begin{pmatrix} \dot{p}_I \\ \dot{\hat{m}}_I \end{pmatrix}.\end{aligned}$$

As in [4], we can rewrite

$$\begin{pmatrix} \dot{p}_I \\ \dot{\hat{m}}_I \end{pmatrix} = \begin{pmatrix} I & 0_{3,3} \\ 0_{3,3} & (\hat{m}_I)_\times^T \end{pmatrix} \dot{x} = M_I \dot{x},$$

and

$$\begin{pmatrix} \dot{p}_E \\ \dot{\hat{m}}_E \end{pmatrix} = \begin{pmatrix} I & 0_{3,3} \\ 0_{3,3} & (\hat{m}_E)_\times^T \end{pmatrix} \dot{\chi} = M_E \dot{\chi},$$

where $(\cdot)_\times : \mathbb{R}^3 \to \mathfrak{so}(3)$ is the *skew operator* and $0_{i,k} \in \mathbb{R}^{i\times k}$ is referred to as the zero matrix.

By taking into account the robot jacobian matrix J, i.e. the matrix for which $\dot{\chi} = J\dot{q}$ [25], we can define

$$J_q = \begin{pmatrix} \frac{\partial \tau}{\partial p} & \frac{\partial \tau}{\partial \hat{m}_E} \end{pmatrix} M_E J$$

and

$$J_x = -\begin{pmatrix} \frac{\partial \tau}{\partial p} & \frac{\partial \tau}{\partial \hat{m}_I} \end{pmatrix} M_I.$$

The force and torque derivative reads, as in (2), as

$$\dot{\tau}_m = J_x \dot{x} + J_q \dot{q}.$$

APPENDIX B
PROOFS OF LEMMAS AND THEOREMS

In the following we provide the proofs of Lemma 1 and Theorem 1.

Proof of Lemma 1: Consider the positive definite Lyapunov function

$$V(\tilde{x}, \dot{\tilde{x}}) = \frac{1}{2}\dot{\tilde{x}}^T B(x)\dot{\tilde{x}} + \frac{1}{2}\tilde{x}^T K_p \tilde{x}.$$

Being $\dot{x}_d = 0$ by assumption, $\dot{\tilde{x}}^T B(x)\dot{\tilde{x}}$ is the kinetic energy of the mechanical system; K_p is positive definite by definition. The time derivative of the chosen Lyapunov function reads as

$$\begin{aligned}
\dot{V}(\tilde{x}, \dot{\tilde{x}}) &= \dot{x}^T B(x)\ddot{x} + \frac{1}{2}\dot{x}^T \dot{B}(x)\dot{x} + \tilde{x}^T K_p \dot{\tilde{x}} \\
&= \dot{x}^T(\tau - C(x,\dot{x})\dot{x} - G(x)) + \frac{1}{2}\dot{x}^T \dot{B}(x)\dot{x} \\
&\quad + \tilde{x}^T K_p \dot{x} \\
&= -\dot{x}^T K_d \dot{x} + \frac{1}{2}\dot{x}^T(\dot{B}(x) - 2C(x,\dot{x}))\dot{x} \\
&= -\dot{x}^T K_d \dot{x}. \\
&= -\dot{\tilde{x}}^T K_d \dot{\tilde{x}}.
\end{aligned}$$

The last two inferences hold for the *work-energy theorem* [25], which implies $\dot{x}^T(\dot{B}(x) - 2C(x,\dot{x}))\dot{x} = 0$, and the fact that $\dot{x}_d = 0$. Being K_d positive definite, by design, $\dot{V}(\tilde{x}, \dot{\tilde{x}}) \leq 0$ and the system is, at least, marginally stable.

One can prove the asymptotic stability by applying the La Salle's theorem. In fact, the set $\Omega = \left\{(\tilde{x}, \dot{\tilde{x}}) | \dot{V}(\tilde{x}, \dot{\tilde{x}}) = 0\right\} = \{(\tilde{x}, 0)\}$ is closed and $V(\tilde{x}, \dot{\tilde{x}})$ is radially unlimited. Moreover, being $\dot{x}_d = 0$ by choice, $\dot{\tilde{x}} = 0$ leads to $\dot{x} = 0$. By substitution in (1), being $\tau = \tau_d$ by assumption, we obtain

$$K_p \tilde{x} = 0,$$

thus, the largest invariant set is $M = \left\{(\tilde{x}, \dot{\tilde{x}}) | K_p \tilde{x} = 0\right\}$. Being K_p positive definite, by definition, $M = \left\{(\tilde{x}, \dot{\tilde{x}}) = (0, 0)\right\}$ and the equilibrium is asymptotically stable. ∎

Proof of Theorem 1: Consider the positive definite Lyapunov function

$$W(\tilde{x}, \dot{\tilde{x}}, \tilde{\tau}) = V(\tilde{x}, \dot{\tilde{x}}) + \frac{1}{2}\tilde{\tau}^T \tilde{\tau},$$

where $V(\tilde{x}, \dot{\tilde{x}})$ is the Lyapunov function defined in the proof of Lemma 1. The time derivative of the chosen Lyapunov function is

$$\begin{aligned}
\dot{W}(\tilde{x}, \dot{\tilde{x}}, \tilde{\tau}) &= \dot{x}^T B(x)\ddot{x} + \frac{1}{2}\dot{x}^T \dot{B}(x)\dot{x} + \tilde{x}^T K_p \dot{\tilde{x}} + \tilde{\tau}^T \dot{\tilde{\tau}} \\
&= \dot{x}^T(\tau - C(x,\dot{x})\dot{x} - G(x)) + \frac{1}{2}\dot{x}^T \dot{B}(x)\dot{x} \\
&\quad + \tilde{x}^T K_p \dot{x} - \tilde{\tau}^T(K\tilde{\tau} - \dot{x}) \\
&= \dot{x}^T(\tau_d - \tilde{\tau} - C(x,\dot{x})\dot{x} - G(x)) + \frac{1}{2}\dot{x}^T \dot{B}(x)\dot{x} \\
&\quad + \tilde{x}^T K_p \dot{x} - \tilde{\tau}^T(K\tilde{\tau} - \dot{x}) \\
&= \dot{x}^T(\tau_d - C(x,\dot{x})\dot{x} - G(x)) \\
&\quad + \frac{1}{2}\dot{x}^T \dot{B}(x)\dot{x} + \tilde{x}^T K_p \dot{x} - \tilde{\tau}^T(K\tilde{\tau} - \dot{x}) \\
&\quad - \dot{x}^T \tilde{\tau} \\
&= -\dot{x}^T K_d \dot{x} + \frac{1}{2}\dot{x}^T(\dot{B}(x) - 2C(x,\dot{x}))\dot{x} \\
&\quad - \tilde{\tau}^T K \tilde{\tau} \\
&= \dot{V}(\tilde{x}, \dot{\tilde{x}}) - \tilde{\tau}^T K \tilde{\tau},
\end{aligned}$$

which is negative semidefinite. The La Salle's theorem can be applied, as in Lemma 1, to show the asymptotic stability of the controlled dynamics. By following the steps of the proof of Lemma 1, one can show that the largest invariant set is found with the same procedure: $N = \{(\tilde{x}, \dot{\tilde{x}}, \tilde{\tau}) | K_p \tilde{x} = 0\}$. Therefore, the asymptotic stability is proved. ∎

REFERENCES

[1] A. Arezzo, A. Menciassi, P. Valdastri, G. Ciuti, G. Lucarini, M. Salerno, C. Di Natali, M. Verra, P. Dario, and M. Morino, "Experimental assessment of a novel robotically-driven endoscopic capsule compared to traditional colonoscopy," *Digestive and Liver Disease*, vol. 45, no. 8, pp. 657–662, 2013. [Online]. Available: http://dx.doi.org/10.1016/j.dld.2013.01.025

[2] P. Valdastri, C. Quaglia, E. Susilo, A. Menciassi, P. Dario, C. Ho, G. Anhoeck, and M. Schurr, "Wireless therapeutic endoscopic capsule: in vivo experiment," *Endoscopy*, vol. 40, no. 12, pp. 979–982, dec 2008. [Online]. Available: http://www.thieme-connect.de/DOI/DOI?10.1055/s-0028-1103424

[3] P. Valdastri, G. Ciuti, A. Verbeni, A. Menciassi, P. Dario, A. Arezzo, and M. Morino, "Magnetic air capsule robotic system: proof of concept of a novel approach for painless colonoscopy," *Surgical Endoscopy*, vol. 26, no. 5, pp. 1238–1246, 2012. [Online]. Available: https://doi.org/10.1007/s00464-011-2054-x

[4] A. W. Mahoney and J. J. Abbott, "Five-degree-of-freedom manipulation of an untethered magnetic device in fluid using a single permanent magnet with application in stomach capsule endoscopy," *The International Journal of Robotics Research*, vol. 35, no. 1-3, pp. 129–147, 2016.

[5] C. Chautems and B. J. Nelson, "The tethered magnet: Force and 5-DOF pose control for cardiac ablation," *Proceedings - IEEE International Conference on Robotics and Automation*, pp. 4837–4842, 2017.

[6] M. N. Faddis, W. Blume, J. Finney, A. Hall, J. Rauch, J. Sell, K. T. Bae, M. Talcott, and B. Lindsay, "Novel, magnetically guided catheter for endocardial mapping and radiofrequency catheter ablation," *Circulation*, vol. 106, no. 23, pp. 2980–2985, 2002.

[7] S. Toggweiler, J. Leipsic, R. K. Binder, M. Freeman, M. Barbanti, R. H. Heijmen, D. A. Wood, and J. G. Webb, "Management of vascular access in transcatheter aortic valve replacement: Part 2: Vascular complications," *JACC: Cardiovascular Interventions*, vol. 6, no. 8, pp. 767–776, 2013.

[8] S. K. Hilai, W. J. Michelsen, J. Driller, and E. Leonard, "Magnetically guided devices for vascular exploration and treatment: Laboratory and clinical investigations," *Radiology*, vol. 113, no. 3, pp. 529–540, 1974.

[9] S. Ernst, F. Ouyang, C. Linder, K. Hertting, F. Stahl, J. Chun, H. Hachiya, D. Bänsch, M. Antz, and K. H. Kuck, "Initial Experience with Remote Catheter Ablation Using a Novel Magnetic Navigation System: Magnetic Remote Catheter Ablation," *Circulation*, vol. 109, no. 12, pp. 1472–1475, 2004.

[10] J. Sikorski, I. Dawson, A. Denasi, E. E. Hekman, and S. Misra, "Introducing BigMag - A novel system for 3D magnetic actuation of flexible surgical manipulators," *Proceedings - IEEE International Conference on Robotics and Automation*, pp. 3594–3599, 2017.

[11] W. J. Casarella, J. Driller, and S. K. Hilal, "The magnetically guided bronchial catheter of modified pod design: A new approach to selective bronchoscopy," *Radiology*, vol. 93, no. 4, pp. 930–932, 1969.

[12] J. Edelmann, A. J. Petruska, and B. J. Nelson, "Magnetic control of continuum devices," *International Journal of Robotics Research*, vol. 36, no. 1, pp. 68–85, 2017.

[13] ——, "Estimation-Based Control of a Magnetic Endoscope without Device Localization," *Journal of Medical Robotics Research*, vol. 03, no. 01, p. 1850002, Mar 2018. [Online]. Available: http://www.worldscientific.com/doi/abs/10.1142/S2424905X18500022

[14] A. J. Petruska and B. J. Nelson, "Minimum Bounds on the Number of Electromagnets Required for Remote Magnetic Manipulation," *IEEE Transactions on Robotics*, vol. 31, no. 3, pp. 714–722, 2015.

[15] C. Chautems, A. Tonazzini, D. Floreano, and B. J. Nelson, "A variable stiffness catheter controlled with an external magnetic field," *2017 IEEE/RSJ International Conference on Intelligent Robots and Systems (IROS)*, pp. 181–186, 2017. [Online]. Available: http://ieeexplore.ieee.org/document/8202155/

[16] T. Greigarn, R. Jackson, T. Liu, and M. C. Çavuşoğlu, "Experimental validation of the pseudo-rigid-body model of the MRI-actuated catheter," in *2017 IEEE International Conference on Robotics and Automation (ICRA)*, May 2017, pp. 3600–3605.

[17] S. Jeon, A. K. Hoshiar, K. Kim, S. Lee, E. Kim, S. Lee, J. Kim, B. J. Nelson, H. Cha, B. Yi, and H. Choi, "A magnetically controlled soft microrobot steering a guidewire in a three-dimensional phantom vascular network," *Soft Robotics*, vol. 0, no. 0, 0, pMID: 30312145. [Online]. Available: https://doi.org/10.1089/soro.2018.0019

[18] S. Yim and M. Sitti, "Design and Rolling Locomotion of a Magnetically Actuated Soft Capsule Endoscope," *IEEE Transactions on Robotics*, vol. 28, no. 1, pp. 183–194, Feb 2012.

[19] P. Ryan and E. Diller, "Magnetic Actuation for Full Dexterity Microrobotic Control Using Rotating Permanent Magnets," *IEEE Transactions on Robotics*, vol. 33, no. 6, pp. 1398–1409, 2017.

[20] G. Ciuti, P. Valdastri, A. Menciassi, and P. Dario, "Robotic magnetic steering and locomotion of capsule endoscope for diagnostic and surgical endoluminal procedures," *Robotica*, vol. 28, no. 02, p. 199, Mar 2010.

[21] A. Z. Taddese, P. R. Slawinski, K. L. Obstein, and P. Valdastri, "Nonholonomic closed-loop velocity control of a soft-tethered magnetic capsule endoscope," in *2016 IEEE/RSJ International Conference on Intelligent Robots and Systems (IROS)*. IEEE, Oct 2016, pp. 1139–1144. [Online]. Available: http://ieeexplore.ieee.org/document/7759192/

[22] M. Miyasaka and P. Berkelman, "Magnetic levitation with unlimited omnidirectional rotation range," *Mechatronics*, vol. 24, no. 3, pp. 252–264, 2014. [Online]. Available: http://dx.doi.org/10.1016/j.mechatronics.2014.02.001

[23] H. K. Khalil, *Nonlinear systems*. Macmillan Pub. Co., 1992. [Online]. Available: https://books.google.co.uk/books?id=RVHvAAAAMAAJ

[24] A. Z. Taddese, P. R. Slawinski, M. Pirotta, E. De Momi, K. L. Obstein, and P. Valdastri, "Enhanced real-time pose estimation for closed-loop robotic manipulation of magnetically actuated capsule endoscopes," *The International Journal of Robotics Research*, vol. 37, no. 8, pp. 890–911, 2018. [Online]. Available: https://doi.org/10.1177/0278364918779132

[25] B. Siciliano, L. Sciavicco, L. Villani, and G. Oriolo, *Robotics: Modelling, Planning and Control*, 1st ed. Springer Publishing Company, Incorporated, 2008.

[26] A. Alazmani, A. Hood, D. Jayne, A. Neville, and P. Culmer, "Quantitative assessment of colorectal morphology: Implications for robotic colonoscopy," *Medical Engineering & Physics*, vol. 38, no. 2, pp. 148 – 154, 2016. [Online]. Available: http://www.sciencedirect.com/science/article/pii/S1350453315002763

[27] A. J. Petruska and J. J. Abbott, "Optimal permanent-magnet geometries for dipole field approximation," *IEEE Transactions on Magnetics*, vol. 49, no. 2, pp. 811–819, Feb 2013.